Polarizable Molecular Mechanics Studies of Cu(I)/Zn(II) Superoxide Dismutase: Bimetallic Binding Site and Structured Waters

Nohad Gresh,*[a] Krystel El Hage,[a,b] David Perahia,[c] Jean-Philip Piquemal,[d] Catherine Berthomieu,[e,f] and Dorothée Berthomieu[g]

The existence of a network of structured waters in the vicinity of the bimetallic site of Cu/Zn-superoxide dismutase (SOD) has been inferred from high-resolution X-ray crystallography. Long-duration molecular dynamics (MD) simulations could enable to quantify the lifetimes and possible interchanges of these waters between themselves as well as with a ligand diffusing toward the bimetallic site. The presence of several charged or polar ligands makes it necessary to resort to second-generation polarizable potentials. As a first step toward such simulations, we benchmark in this article the accuracy of one such potential, sum of interactions between fragments Ab initio computed (SIBFA), by comparisons with quantum mechanics (QM) computations. We first consider the bimetallic binding site of a Cu/Zn-SOD, in which three histidines and a water molecule are bound to Cu(I) and three histidines and one aspartate are bound to Zn(II). The comparisons are made for different His6 complexes with either one or both cations, and either with or without Asp and water. The total net charges vary from zero to three. We subsequently perform preliminary short-duration MD simulations of 296 waters solvating Cu/Zn-SOD. Six representative geometries are selected and energy-minimized. Single-point SIBFA and QM computations are then performed in parallel on model binding sites extracted from these six structures, each of which totals 301 atoms including the closest 28 waters from the Cu metal site. The ranking of their relative stabilities as given by SIBFA is identical to the QM one, and the relative energy differences by both approaches are fully consistent. In addition, the lowest-energy structure, from SIBFA and QM, has a close overlap with the crystallographic one. The SIBFA calculations enable to quantify the impact of polarization and charge transfer in the ranking of the six structures. Five structural waters, which connect Arg141 and Glu131, are endowed with very high dipole moments (2.7–3.0 Debye), equal and larger than the one computed by SIBFA in ice-like arrangements (2.7 D).

DOI: 10.1002/jcc.23724

Introduction

Superoxide dismutase (SOD) is a bimetallic (Cu/Zn) enzyme which catalyzes the dismutation of O_2^- radical into dioxygen and hydrogen peroxide.[1] Cu/Zn-SODs are ubiquitous and essential to prevent the effect of oxidative stress in aerobic cells. Alteration of Cu/Zn-SOD has been associated with a number of diseases as familial amyotrophic lateral sclerosis. In addition, Cu/Zn-SOD is differentially expressed in various forms of cancer. The high level of reactive oxygen species (ROS) present in cancer cells renders them highly sensitive to alterations of ROS detoxification systems. Disabling antioxidant mechanisms seems promising to trigger ROS-mediated cell death in cancer cells.[2] Cu/Zn-SOD was notably evidenced as a target of inhibitors from non-small-cell lung cancer cells.[3,4]

The structure of Cu/Zn-SOD is known from high-resolution X-ray crystallography in the oxidized and reduced states.[5,6] The Cu(II) is coordinated to four histidines (His) arranged in a distorted tetragonal shape.[6–8] A water molecule forms a Cu(II) pseudo-ligand, and one histidine (His61) acts as a bridging ligand between Cu(II) and Zn. The other ligands of Zn are two histidines and a monodentate aspartate. Superoxide dismutation is accompanied by the change in redox state of the Cu active site. Superoxide oxidation induces the reduction of $Cu^{[2]+}$ and the rupture of the Cu—His61—Zn bridge.[5,6] A water molecule is located at 3.5–4 Å of Cu(I) stabilized by a 3 Å hydrogen bond to His61 [5, (Fig. 1)]. One specificity of Cu/Zn-SOD's is their equivalent efficiency for both reactions of

[a] N. Gresh, K. El Hage
Chemistry and Biology, Nucleo(s)tides and Immunology for Therapy (CBNIT), UMR 8601 CNRS, UFR Biomédicale, Paris, France
E-mail: nohad.gresh@parisdescartes.fr
[b] K. El Hage
Unité de Biochimie, Université Saint-Joseph, Beirut, Lebanon
[c] D. Perahia
Laboratoire de Biologie et Pharmacologie Appliquée (LBPA), UMR 8113, Ecole Normale Supérieure, France
[d] J.-P. Piquemal
Laboratoire de Chimie Théorique, Sorbonne Universités, UPMC, UMR7616 CNRS, Paris, France
[e] C. Berthomieu
CEA, DSV, IBEB, Laboratoire des Interactions Protéine-Métal, Saint-Paul-lez-Durance, France
[f] C. Berthomieu
CNRS, UMR Biologie Végétale et Microbiologie Environnementale, Saint-Paul-lez-Durance, France
[g] D. Berthomieu
Institut Charles Gerhardt, UMR 5253, CNRS-UM2-UM1-ENSCM, 8 rue de l'Ecole Normale, 34296, Montpellier Cedex 5, France

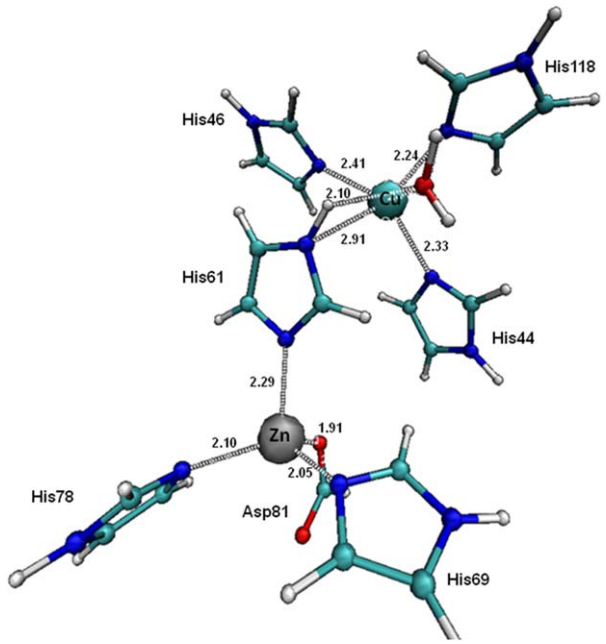

Figure 1. Representation of the bimetallic Cu(I)/Zn(II) binding site.

superoxide reduction and oxidation.[9,10] Cu/Zn-SOD are characterized by a very high reaction rate with superoxide (2×10^9 M s^{-1}), near the diffusion rate of superoxide, which is independent of pH in a large pH range.[11,12] A channel across the protein leads toward the fifth axial coordination of the buried redox Cu. The crystallographic structures of oxidized and reduced Cu/Zn-SOD evidenced a network of ordered water molecules, including the water pseudo-ligand of Cu(II).[5,13] The high resolution structure of reduced Cu(I), Zn-SOD recorded at 100 K[5] revealed 11 structured water molecules arranged in two chains extending toward the protein surface and involving hydrogen bonding with backbone carbonyls as well as interactions with Arg141 and Thr 135 side chains.[5] The water molecules are thought to play a determining role in protonation events associated with superoxide reduction into hydrogen peroxide. Proton transfer routes were, however, not clearly identified. In addition, experimental data demonstrated the critical role of an electrostatic network with a positive gradient formed by positively charged residues, notably the highly conserved Arg141, and polar groups to steer the anionic superoxide toward the Cu.[14–16] The role of the well-ordered water molecules in the electrostatic guidance of superoxide is not clear. Finally, the docking site of superoxide is still debated, and a better understanding of their charge distribution and properties of the water molecules in the superoxide access channel could be of primary importance to clarify these issues.

Cu/Zn-SOD's have been the object of previous molecular dynamics (MD) simulations in the context of classical potentials.[17,18] In line with these studies, and as a preliminary step toward docking of small molecules such as CN^-, N_3^-,[19,20] photosensitizing agents,[21] or inhibitors,[3] in this study we investigate the structures, interaction energies, and electronic properties of structural waters in the vicinity of the Cu/Zn binding site of SOD. This is motivated by previous studies on the binding of inhibitors to a kinase[22] and to a Zn-metalloenzyme[23] target, undertaken with the sum of interactions between fragments Ab initio computed (SIBFA) polarizable potential showing that it is indispensable to account for the presence of highly polarized structural water molecules. These waters can mediate the interactions of the inhibitor with residues of the recognition site. Energy balances in which solvation was accounted for solely by a Continuum reaction field procedure failed to rank properly competing inhibitors in terms of relative binding affinities, while explicit inclusion of the structured water along with continuum solvation enabled to recover the correct ranking.[22] The polarization contribution to the interaction energy, which is absent from classical potentials, was found to be critical to enable for the correct ranking. Along these lines, we resort in this study to the X-ray structure of Cu(I)/Zn(II) form of SOD as a starting point. We first perform comparisons between SIBFA and quantum mechanics (QM) bearing on the bimetallic SOD binding site, in which six His and one Asp residue and one water molecule ligate the cations. Six combinations are considered, having either one, or both, cations, and either with or without Asp and water; their overall net charges thus vary from zero to three. A model of complete SOD including 296 cristallographic waters is then considered. Short-time molecular dynamics (10–20 ps) at different temperatures (>10 and ≤ 300 K) on the water positions were performed to explore the potential energy surface. Six structures along the trajectories are selected and energy-minimized to generate six alternative water networks. It is to be underlined that much longer trajectories than those reported in Refs. [17,18] and *a fortiori* in this work, might have to be considered to quantify the lifetimes, exchange rates of each individual water of the network, and their coexistence with a ligand diffusing toward the binding site. These should be enabled by the advent of a highly efficient and N-scalable code to perform anisotropic polarizable MM and MD (APMM/APMD) simulations over the nanosecond limit [Piquemal et al., in preparation]. In the prospect of such simulations, it is essential to evaluate the accuracy of the SIBFA potential as compared to *ab initio* QM, and this will be done on the six selected structures. The enlarged complexes include the Cu(I)/Zn(II) bimetallic site, protein residues surrounding this site, and the water networks extending beyond the waters identified by X-ray crystallography. There is no precedent to our knowledge for QM/APMM comparisons on complexes having such a large size, totaling 301 atoms. Such validations are the primary objective of this work.

Methods

In the SIBFA procedure, the interaction energy is computed as a sum of five contributions:

$$\Delta E_{tot} = E_{MTP} + E_{rep} + E_{pol} + E_{ct} + E_{disp}$$

which are the electrostatic multipolar, the short-range repulsion, the polarization, the charge transfer, and the dispersion contributions.

We denote by ΔE the energies in the absence of E_{disp}, and by $E1$ and $E2$ the summed first- and second-order contributions, namely $E1 = E_{MTP} + E_{rep}$ and $E2 = E_{pol} + E_{ct}$, respectively.

The starting coordinates of SOD were taken from the high-resolution X-ray structure of monomer B of Cu(I)/Zn(II) bovine SOD[5] (PDB entry 1Q0E), which also enabled to locate the structured waters. We have preferentially resorted to it because of its high resolution (1.15 Å), and its identification of one Cu atom in its reduced form Cu(I). The residue numbering is the same as for monomer B. The H atoms were positioned with the Accelrys package.[24] Solvation was completed to 296 waters with the help of the "discrete" algorithm[25] which locates waters around the accessible hydrophilic sites of a given solute by energy-minimization with a simplified energy potential. The molecular dynamics were done using the velocity-Verlet algorithm[26] which was implemented in the SIBFA code. While the present version has not been released, the SIBFA potential is currently implemented in a highly parallel version of the Tinker code [Piquemal et al., in preparation], destined for a release in a near future.

We used a "lighter" version of the SIBFA potential, in which the charge-transfer contribution is not included. The future availability of its analytical gradients [Narth et al., in preparation] will enable an explicit inclusion of this contribution in MD. On computing E_{pol}, we did not perform iterative calculations on the dipoles either. As discussed below, this will also be remedied by inclusion of its derivatives in the context of an innovative conjugate-gradient minimization method.[27] This is not considered critical in this work, since in the prospect of long-duration MD simulations, we presently seek to generate alternatives to the starting X-ray structure and evaluate if their rankings in terms of relative stabilization energies are plausible as compared to QM calculations. And such structures are those obtained from energy-minimization (EM) on the MD-generated poses with the full SIBFA potential.

The water geometry (OH distance of 0.957 Å, HOH angle of 104.5) was constrained by the SHAKE[28] algorithm. The temperature was controlled by the Berendsen method.[29] Temperatures in the range 10–300 K were considered. For all simulations, the X-ray structure of Cu(I)/Zn(II) SOD was used as a starting point. The time-step was 0.75 fs. This is not considered critical in this work, since in the prospect of long-duration MD simulations we presently seek to generate alternatives to the starting X-ray structure and evaluate if their rankings in terms of relative stabilization energies is plausible as compared to QM calculations. Such structures are those obtained from EM on the MD-generated poses with the full SIBFA potential. Temperatures in the range 10–300 K were considered. The X-ray structure of the Cu(I)/Zn(II) SOD was used as a starting point. We performed six independent simulations of an average duration of 15 ps. The waters were confined by a spherical quadratic potential centered around Cu+ and with a radius of 22 Å. During MD, the protein was not relaxed. In the selected snapshots, the closest 64 waters to the Zn/Cu site were retained and submitted to energy-minimization using the "Merlin" minimizer.[30] Together with Cu(I) and Zn(II), the side-chains of the following residues were relaxed: His44, His46, Thr56, Ser57, Ala58, His61,His69, His78, Asp81, His118, Lys134, Thr135, Asn137, Ser140, and Arg141. No implicit solvation was considered during MD or EM.

As in our preceding studies,[22,23] the distributed multipoles and polarizabilities of the library of fragments used to assemble Cu/Zn-SOD were those previously derived from their molecular orbitals (MO) by the procedures due to Vigné-Maeder and Claverie[31] and to Garmer and Stevens,[32] respectively. The MO's were computed using the CEP 4–31G(2d) basis set.[33] This basis set was also the one used in the density functional theory (DFT) studies of Ref. [18]. The energy decomposition analyses were done with the reduced variational space (RVS) method due to Stevens and Fink[34] as coded in the GAMESS software.[35] The DFT calculations were done with the B97-D and B97-D3 functionals due to Grimme et al.[36,37] and coded in the G09 software.[38] Basis set superposition error (BSSE) effects are evaluated in the course of the RVS analysis on the virtual orbitals using the Boys and Bernardi method.[39] The SIBFA calculations on the model complexes as well as the QM validation calculations were performed without implicit solvent.

Illustrations of the electron density redistribution resulting from the intermolecular interactions were done using the Non-covalent Interaction (NCI) procedure with the NCI-Plot program.[40]

Results and Discussion

Cu(I)/Zn(II) bimetallic binding site. Validation of the intermolecular interaction energies

Prior to investigating the water networks, it was important to evaluate first the accuracy of SIBFA as compared to QM regarding the metal active site of Cu/Zn-SOD. Along with the two metal cations, it is made out of six His residues, one Zn-bound Asp residue, and a Cu-bound water. As in our preceding papers,[23,41,42] the His and Asp residues are represented by imidazole and formate, respectively. The binding site is shown in Figure 1. Zn(II) has the same tetracoordination as with the oxidized form of Cu.[13] Cu(I) is coordinated to three His residues, His44, His46, and His118. Similar to Cu(II), but no longer to His61, due to the protonation of the Nε nitrogen of His61. A water molecule which acted as the fifth Cu(II) ligand[13] has been displaced on passing to reduced Cu(I). However, the equilibrium distance we found is 2.87 Å. This is too long to be considered as part of Cu(I) coordination, but nevertheless smaller than the 3.7 Å distance found by X-ray diffraction.[5] It could be mentioned that a distance of 2.56 Å was also given in Ref. [13] and attributed to a minor form of Cu(II)-complexed SOD. Such a distance is nevertheless itself larger than the 2.19 Å distance found when the oxidized state is predominant.[13] MD with longer simulation times and the complete SIBFA potential should hopefully enable to clarify, in the context of this potential, the outcome of Cu(I) preferential coordination distances and the possible breathing modes around equilibrium distances.

We have considered six distinct complexes, denoted as a–f. The first three ones have only the imidazole ligand complexing either Cu(I) (a) or Zn(II) (b) individually, or both Cu(I) and Zn(II) (c). The fourth to sixth have in addition formate and water,

Table 1. Cu(I)/Zn(II) binding site.

	Cu-His6		Zn-His6		Cu-Zn-His6	
	QC	SIBFA	QC	SIBFA	QC	SIBFA
Ec/EMTP	−95.7	−105.2	−230.7	−238.2	−243.2	−254.5
Eexch/Erep	48.5	53	65.3	72	108.4	112.8
E1	−47.2	−52.3	−165.4	−166.2	−134.8	−141.7
Epol(Cu)	−4	−4.1			−4.5	−4
Epol(RVS)/Epol*	−37.3	−30.9	−146	−133.3	−178.4	−157.8
Epol(VL)/Epol	−32.4	−29.6	−119.2	−115.1	−155.3	−141.4
Ect(Cu->Lig)	−1.5	−2.2			−1.5	−1.8
Ect	−10.8	−9	−32.9	−24.2	−39.7	−33
BSSE	−4.1		−3.3		−5.9	
DE(RVS)/DE(SIBFA)	**−90.3**	**−90.9**	**−314.5**	**−305.6**	**−323.3**	**−316**
DE(HF)	**−94.4**		**−317.5**		**−329.2**	
DE(B97D)/DEtot(SIBFA)	**−142.3**	**−122.9**	**−372.5**	**−335.2**	**−416.2**	**−369.5**
DE(B97D3)	**−144.1**		**−373.6**		**−418**	
DE(MP2)	**−144.6**		**−363.3**		**−400**	
DE(B97D3) augcc-pvtz	**−133.5**		**−361.3**			

	Cu-His6-Asp-H2O		Zn-His6-Asp-H2O		Cu-Zn-His6-Asp-H2O	
	QC	SIBFA	QC	SIBFA	QC	SIBFA
Ec/EMTP	−114.1	−127.8	−512.2	−524.9	−584.4	−601.2
Eexch/Erep	62	73.4	124.1	132.8	168.7	174.4
E1	−52.2	−54.4	−388.1	−392.1	−415.7	−426.8
Epol(Cu)	−3.5	−3.2			−3.8	−3.3
Epol(RVS)/Epol*	−52.3	−46.6	−131.9	−132.3	−161.7	−144.4
Epol(VL)/Epol	−52.1	−41.1	−109.1	−96.9	−138.4	−119.2
Ect(Cu->Lig)	−1.5	−2.6			−1.5	−2.1
Ect	−11.5	−10	−31.8	−27.7	−40.5	−36.5
BSSE	−7.8		−7.4		−9.7	
DE(RVS)/DE(SIBFA)	**−107.9**	**−105.5**	**−521.6**	**−516.3**	**−584.9**	**−582.5**
DE(HF)	**−115.7**		**−529**		**−594.6**	
DE(B97D)/DEtot(SIBFA)		**−146.7**	**−587.8**	**−563.5**	**−687.4**	**−654.8**
DE(B97D3)			**−590.3**		**−690.7**	
DE(B97D3)/augcc			**−569.2**			

Values of the SIBFA and QM intermolecular interaction energies and their individual contributions.
*The polarization energy computed in SIBFA with the permanent multipoles prior to iteratively including the effects of the induced dipoles.

complexing either Cu(I) (d) or Zn(II) individually (e), or both (f). The QM intermolecular interaction energies are seen to have values in the range −90 to −580 kcal/mol. How well could APMM match the QM interaction energies over such a range, as concerns both ΔE and its individual contributions? A closely related issue relates to the second-order contributions, E_{pol} and E_{ct} and whether, owing to their strong nonadditive characters in such complexes[41–44] their evolutions can remain controlled in the diverse complexes, the net charge of which can vary from zero (complex d) to three (complex c).

Such complexes also enable to verify, if the Cu(I) polarization contribution computed with SIBFA with dipolar and quadrupolar polarizabilities[45] can stably match E_{pol}(Cu) from RVS in complexes a, c, d, and f. The results are reported in Table 1, which lists the intermolecular interaction energies and their components. For each complex, the RVS and SIBFA results are reported on two successive columns. Consistent with results published in previous articles,[41–45] ΔE(SIBFA) can match closely ΔE(RVS). The relative errors are less than 2% in four out of the six complexes and 3% in two ones, b and c. There are nevertheless some compensation of errors, notably regarding Coulomb energy (EC), which is slightly overestimated by E_{MTP}, and E_{pol}, which is underestimated in SIBFA. Similar effects were previously reported[41,42] but never prevented close agreements between the SIBFA and QM total interaction energies, the relative errors being <3%. It is also seen that E_{pol} (Cu) for SIBFA, which is dominated by the quadrupolar polarizability, matches closely E_{pol} (Cu) from RVS in all four Cu complexes. The charge transfer from Cu(I) to its ligands has a relatively small value of approximately 2 kcal/mol which also appears consistent with the RVS results.

There are larger QM-SIBFA differences on passing to the correlated level. For complexes a–c, ΔE_{tot}(SIBFA) is smaller in magnitude than ΔE(B97-D) by amounts in the range 22–47 kcal/mol out of 140–416 kcal/mol. On the one hand, this could be

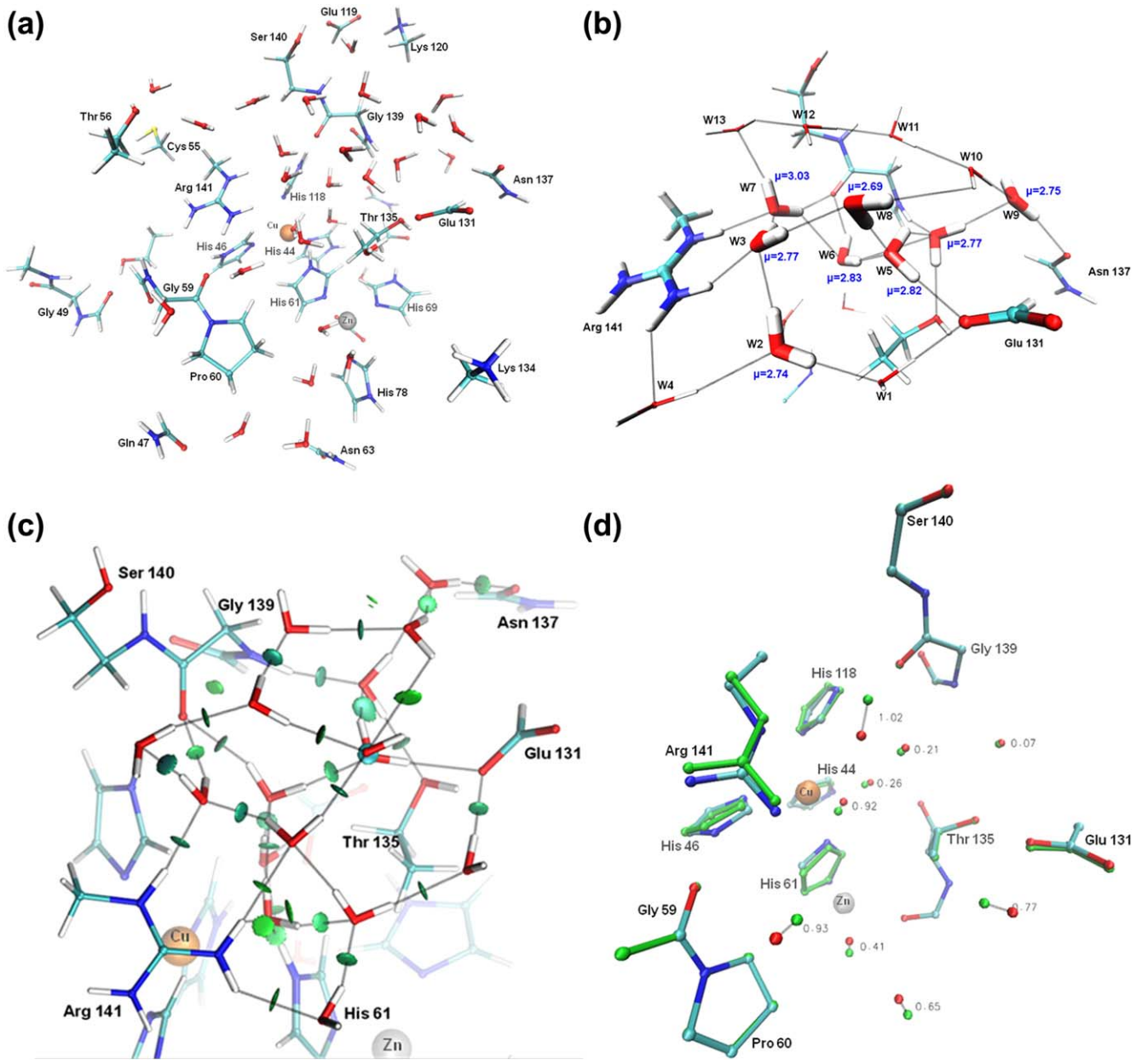

Figure 2. a) Representation of complex "c" encompassing 300 atoms; b) close-up on the most-stably bound waters; c) NCI contours around the most-stably bounds waters; and d) superimposition of the most-stably bound waters with the waters identified in the X-ray structure.

due to some deficiency in the calculation of E_{disp} when metal cations are involved. On the other hand, it could also be due to some overestimation of the gain due to correlation by the B97-D or B97-D3 functionals with the CEP 4–31G(2d) basis set.

We, thus, redid the B97-D3 computations for complexes a–c with the augcc-pvtz basis set. ΔE(B97-D3) is about 10 kcal/mol smaller in magnitude than with the CEP 4–31G(2d) basis set, and is accordingly closer to ΔE_{tot}(SIBFA). There is an additional indication that ΔE(B97-D3) could be somewhat overestimated in the polyligated complexes of metal cations, and more so with the CEP 4–31G(2d) basis set than with the augcc-pvtz one. It relates to the fact that ΔE(MP2/CEP 4–31G(2d)) is actually smaller in magnitude than ΔE(B97-D3) in the case of the Zn(II) complexes b and c [and equal to it in the case of the Cu(I) complex a]. Yet ΔE(MP2) has consistently been reported to overestimate the "true" correlated intermolecular interaction energies.[46] Nevertheless, such caveats should only have a limited impact for this study as shown below, they do not affect significantly the relative energy differences between the competing networks of structural waters.

Structured waters

The six model complexes a, b, c, d, e, and f which were extracted from the energy-minimized MD poses and used for comparison with QM have a total of 301 atoms. Along with the two metal cations, they encompass: the main-chain of the following residues: Gly49-Asp50; Pro60; Gly139; Ser140; the side-chains of His44, His46, Gln47, Cys55, Thr56, His61, Asn63, His69, His78, Asp81, Asn84, Thr114, His118, Glu119, Lys120,

Table 2. Complexes "a" to "f."

	a	b	c	d	e	f
DE(HF)	**−1139.7**	**−1162.7**	**−1178.6**	**−1130.7**	**−1123.6**	**−1150.6**
E1+E2	**−1109.2**	**−1135.2**	**−1146.1**	**−1105.1**	**−1087.2**	**−1129.2**
EMTP	−1284.8	−1363	−1361.5	−1285	−1310.5	−1345.6
Erep	495.3	571.6	556.4	498.4	540.5	559.3
E1	−789.5	−791.5	−805.1	−786.6	−770	−786.3
Epol	−231	−246.5	−245	−229	−228	−244
Ect	−76.9	−87.8	−86.2	−79.1	−80.6	−88.1
Epol(Cu+)	−8.9	−6.6	−7.1	−7.7	−5.3	−7.9
Ect(Cu->Lig)	−2.8	−2.8	−2.7	−2.7	−2.9	−2.8
dEcorr	−225	−257.6	−253.8	−212.9	−252.8	−254.6
DE(B97d)	**−1364.7**	**−1420.3**	**−1432.4**	**−1343.6**	**−1376.4**	**−1405.2**
Edisp	−202.6	−238.1	−234	−196.4	−234.1	−232.2
DE tot	**−1311.8**	**−1373.2**	**−1380**	**−1301.5**	**−1321.3**	**−1361.4**

Compared QM and SIBFA intermolecular interaction energies.

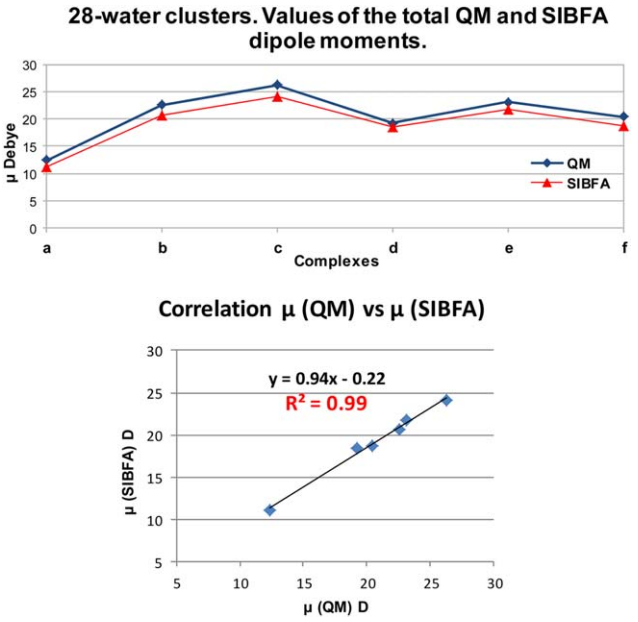

Figure 3. Compared evolutions of the total dipole moments in the 28-water clusters in structures "a"–"f". [Color figure can be viewed in the online issue, which is available at wileyonlinelibrary.com.]

Asp122, Glu131, Lys134, Thr135, Asn137, Ser140, and Arg141; and a total of 28 waters. The lowest energy-structure labeled c is represented in Figure 2a. A dense array is found between two ionic residues, Glu131 and Arg141, which are located beneath the bimetallic site and are separated by a distance of 10 Å between their gamma and epsilon carbons. These residues are connected by several water networks. Thus, starting from Glu131, the first network involves W1, W2, and W3, and another one involves W4 instead of W3 (Fig. 2b). W4 binds to the edge of Arg141. A third network involves W5, W6, and W7, and a fourth has again W5, then W8 and again W3 which also donates a proton to W7. W3 is thus fully involved in three networks, acting as an H-bond acceptor from Arg141 and W2, and as a bond donor to W7 and W8. The water networks are also channeled in other regions in the vicinity. There is, thus, an extended linear network of six waters at the periphery of the W5–W7 network. The first water donates a proton to the side-chain of Asn137 and the sixth accepts a proton from the side-chain of Thr56 while the last accepts a proton from W7. This network connects to the dense network between Arg141 and Glu131 through three water molecules. A five-water network connects the side-chains of Asn63, Asn47, and the main-chain of Lys134. In addition, His61 donates its NH proton to two water molecules. The first water connects it by a three water network to Arg141. The second water connects it by a two-water network to Glu131 and by a three-water network to Gly139. Thr135 donates a proton to Glu131 and accepts a proton from a water molecule which is involved in three additional interactions: as a proton acceptor from the NH of Gly139 and from a Glu131-bound water, and as a proton donor to the Asn137-bound water (Fig. 2b).

A close-up of the networks between Arg141 and Gu131 is given in Figure 2b.

Six waters have dipole moments larger than that of ice, which amounts to 2.70 Debyes in the context of SIBFA. Waters W5, W6, and W7 of the third network are those having the highest dipole moments amounting to 2.82, 2.83, and 3.03 Debye, respectively. There is a precedent to such unusually high μ values, which was published in a study of structured water molecules in the recognition of FAK kinase.[22] These waters similarly mediated the interactions between ionic residues of FAK as well as with the ionic moiety of the inhibitor. Such a situation is in fact likely to be a general one and attests to the onset of very strong polarization effects in charged recognition sites and in their vicinity. Figure 2c gives the NCI contours and Figure 2d is a superimposition of the energy-minimized waters with the structured waters found by X-ray diffraction. Nine structural waters are at positions at distances 1 Å and less from the positions occupied by crystallographic waters. There are five residues which on the basis of X-ray crystallography were found to bind to structural waters, namely Thr56, His61, Thr135, Gly139, and Arg141.[5] This survey is fully consistent with such involvements, but underlines in addition the strong role of Glu131. In line with these X-ray results, it supports the involvement of aminoacids beyond the sole Cu and Zn-coordinating ones. Thus, an enlarged SOD recognition site should be considered. It would encompass

Table 3. Complexes "a" to "f."

	a	b	c	d	e	f
DE(HF)	**−219.5**	**−238**	**−263.5**	**−216.8**	**−211.4**	**−237.8**
DE(SIBFA)	**−213.6**	**−243.1**	**−255.4**	**−214**	**−201.7**	**−240**
E1	−130.2	−132.2	−146.8	−126.7	−116.1	−129.2
E2	−83.4	−110.9	−108.6	−87.3	−85.6	−110.8
DE(B97d)	**−315**	**−377.2**	**−389.2**	**−301.3**	**−335.4**	**−363.7**
DEtot(SIBFA)	**−307.9**	**−374.4**	**−383**	**−303.8**	**−329.1**	**−365.7**

Compared QM and SIBFA stabilization energies due to the 28 water molecules.

residues such as Gln47, Gly 49, Thr56, Gly49-Asp50; Pro60; Gly139; Ser140; the side-chains of His44, His46, Gln47, Cys55, Thr56, His61, Asn63, His69, His78, Asp81, Asn84, Thr114, His118, Glu119, Lys120, Asp122, Glu131, Lys134, Thr135, Asn137, Ser140, and Arg141; Asn63, Glu131, Asn137, Lys139, Arg141. The structural waters bound to them are to be considered as well, as an integral part of the site.

Figures and descriptions of the five other water networks in the complexes a, b, d, f, and e with the SOD recognition metal active site are given in Supporting Information 1. At this point, we would like to mention that despite the short simulation times, these structures appear sufficiently well differentiated from one another in terms of their hydrogen-bonding networks, stabilization energies (Tables 2 and 3) and total dipole moments (Fig. 3). Even when the structure differences were limited, as between complexes b and c, the corresponding QM energy differences could be accounted for.

An indirect validation for the computed dipole moments can be done on comparing the SIBFA values of the total dipole moments in representative complexes to the corresponding QM ones. These values represent the sums of permanent and induced dipoles on all individual fragments, so that errors on these could severely impact the final sum. In fact, the comparison with QM results is only rigorously valid for neutral entities, as the dipole moment of any non-neutral molecular fragment is not translation independent. In fact, even for complexes with a net charge of zero, the individual QM fragments may not be neutral due to interfragment charge-transfer effects. Keeping this reservation in mind, we have considered the six neutral 28-water clusters extracted from recognition sites a–f and compared their total QM and SIBFA dipole moments. The total SIBFA dipole moments evolve with a good parallelism to the QM ones and the numerical values are close (Fig. 3). An unexpected feature relates to the strong sensitivity of μ to the structure of the complex, as it passes from 12.4 and 11.1 D by QM and SIBFA, respectively, in complex "a", to 26.3 and 24.1 D (QM and SIBFA, respectively) in complex "c". For completeness, we have also considered the entirety of the model complexes but removed the two farthest Lys residues, Lys120, and Lys134, to have a complex with a null net charge even though several residues are charged. The corresponding figure is given as Supporting Information 2. Even in this extreme case and considering the above reservation, the SIBFA curve retains a satisfactory parallelism to the QM one, even though the values of μ have increased by factors of 3–4 with respect to complex "c" of the "bare" water cluster considered above.

The recognition site has a total of 301 atoms. Together with to the two metal cations, it has four anionic residues and three cationic ones, and several polar residues, namely six imidazoles and six formamides. In addition, there are highly structured waters networks in six distinct and competing arrangements. Could then a meaningful agreement of SIBFA with QM still be obtained regarding both the magnitudes of ΔE and their ranking? For this evaluation, we have performed single-point Hartree-Fock (HF) and DFT computations on the SIBFA energy-minimized structures. The results are reported in Table 2, which lists the values of the interaction energies and those of the SIBFA contributions.

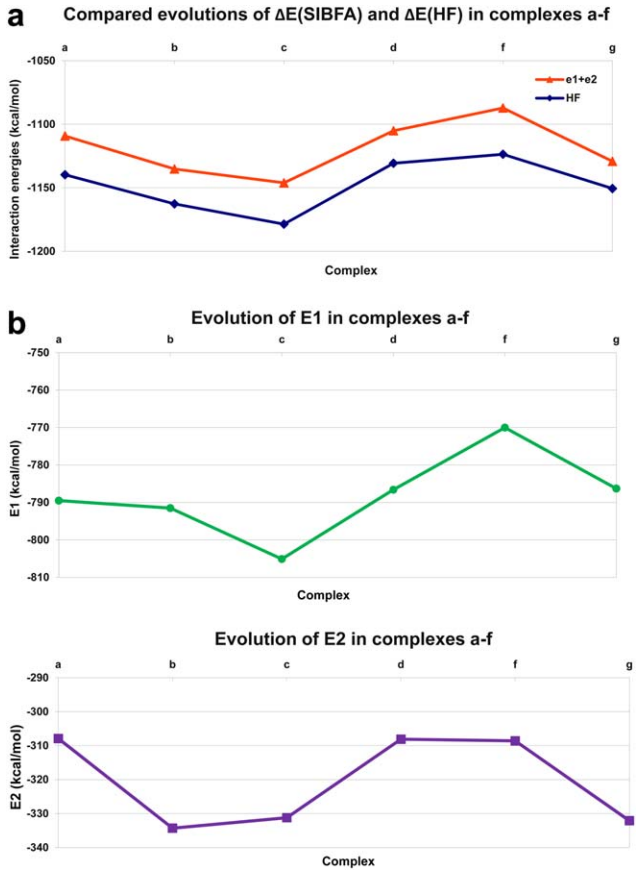

Figure 4. a) Compared evolutions of ΔE(SIBFA) and ΔE(HF) in structures "a"—"f"; and b) evolutions of $E1$ and $E2$ in structures "a"–"f". [Color figure can be viewed in the online issue, which is available at wileyonlinelibrary.com.]

We first comment the results obtained in the absence of the SIBFA E_{disp} contribution. The values of ΔE(SIBFA) can match very closely those of ΔE(HF), the relative error being 3%, which would actually be reduced further if the BSSE correction were taken into account.

The summed second-order terms, $E2$, amounts to 30% of ΔE(SIBFA). The parallelism between SIBFA and QM values is

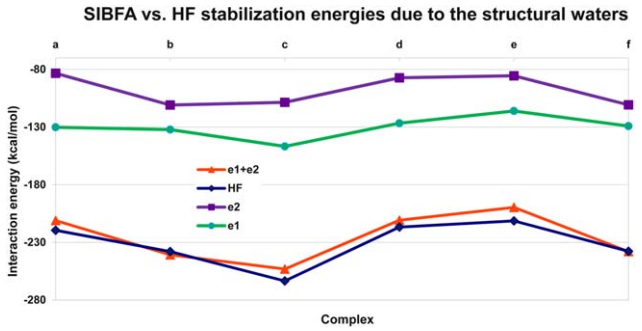

Figure 5. Stabilization brought by the 28 waters. Compared evolutions of ΔE(SIBFA) and ΔE(HF); and corresponding separate evolutions of $E1$ and $E2$. [Color figure can be viewed in the online issue, which is available at wileyonlinelibrary.com.]

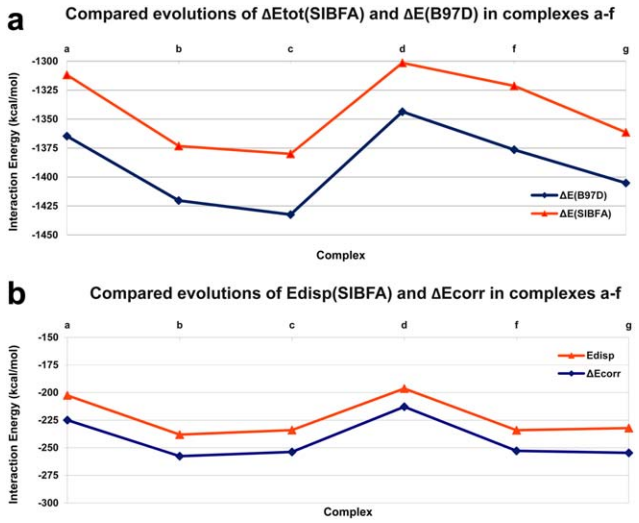

Figure 6. a) Compared evolutions of ΔE_{tot}(SIBFA) and ΔE(B97-D); and b) evolutions of E_{disp} and ΔE_{corr}. [Color figure can be viewed in the online issue, which is available at wileyonlinelibrary.com.]

illustrated in Figure 4a. Figure 4b reports the separate evolutions of *E*1 and *E*2. Neither *E*1 nor *E*2 taken alone can match the evolution of ΔE(QM).

Another test concerns the stabilization energy contributed by the 28 waters. For each structure, and for both SIBFA and QM, it was computed as the difference between the solvated and unsolvated complexes at the same geometry. The results are reported in Table 3. The corresponding evolutions are plotted in Figure 5, along with those of *E*1 and *E*2. The evolution of ΔE(SIBFA) again closely matches that of ΔE(HF) (Fig. 5). Consideration of the separate trends of *E*1 and *E*2 (SIBFA), also reported in Figure 5, is instructive: none of the two curves alone can match the trends of ΔE(HF), but each needs to be complemented by the other to enable such a match. This can be visually seen on passing from complex "a" to complex "b", when *E*1 has a near flat behavior, in marked contrast to *E*2. Conversely, on passing next from "b" to "c", it is now *E*2 that has a near flat behavior, and it is *E*1 that confers its shape to ΔE. An important asset to account properly for the magnitude of E_{pol} and its cooperativity in water networks is the use of off-centered polarizabilities on the localized sp3 lone pairs of the oxygens, as previously shown by some of us.[47]

Table 2 also lists the correlated QM intermolecular energy values computed with the B97-D functional, ΔE(B97-D), along with the gain in interaction energies, ΔE_{corr}, on passing from the HF to the B97-D level. The corresponding SIBFA values, ΔE_{tot} and E_{disp}, are listed next. There is a rather constant offset of app. 50 kcal/mol out of 1400, that is, 4%, between ΔE_{tot} and ΔE(B97). It translates to a large part an app. 30 kcal/mol offset between ΔE and ΔE(HF). The ΔE(HF) values of Table 2 are uncorrected for BSSE due to the size of the complexes and the large number of individual fragments, namely 50. An additional offset is the one between E_{disp} and ΔE_{corr}, which amounts to 20 kcal/mol. The latter appears to be due to a large part to the one observed at the bimetallic site (Table 1). Yet it was observed that in such a site, ΔE(B97-D) had even larger magnitudes than ΔE(MP2), which is considered to be an upper bound for the magnitude of ΔE. Figures 6a and 6b report, respectively, the compared evolutions of ΔE_{tot}(SIBFA)

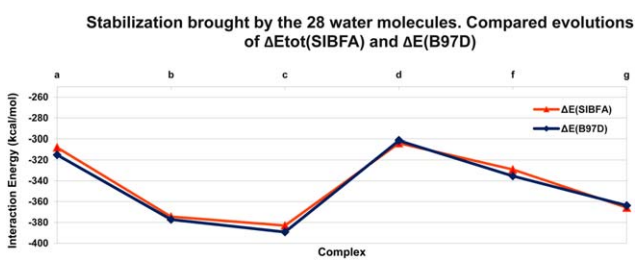

Figure 7. Stabilization brought by the 28 waters. Compared evolutions of ΔE_{tot}(SIBFA) and ΔE(B97-D). [Color figure can be viewed in the online issue, which is available at wileyonlinelibrary.com.]

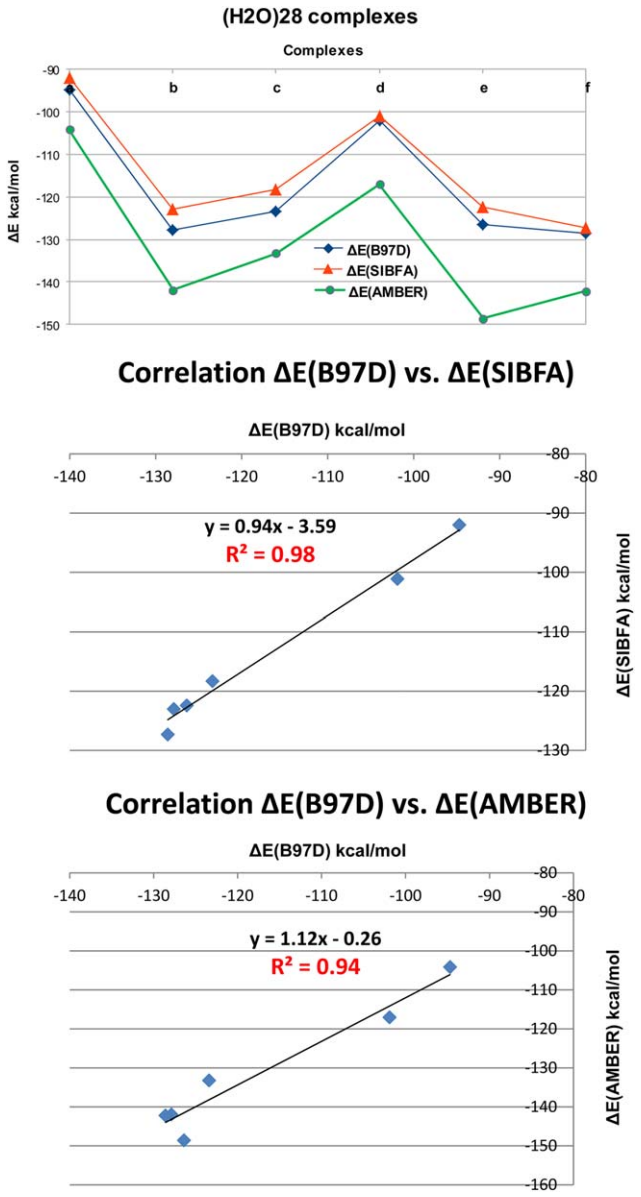

Figure 8. Compared evolutions of the B97-D, SIBFA, and AMBER interaction energies in the six 28-water clusters. [Color figure can be viewed in the online issue, which is available at wileyonlinelibrary.com.]

and of ΔE(B97-D), and those of E_{disp} and ΔE_{corr}. A striking parallelism between the SIBFA and the QM curves can be observed in both figures. The evolutions of the relative stabilizations brought by the water molecules, computed in terms of ΔE_{tot}(SIBFA) and ΔE(B97-D), are compared in Figure 7. The curves are nearly superimposable, and the numerical agreement is even better than between ΔE(SIBFA) and ΔE(HF), namely down to 2%. The offsets concerning correlation effects in the bimetallic binding site appear to have been purged.

Following a proposal by a reviewer, we have also performed a comparison with a classical force-field, AMBER.[48] Here, again we have limited ourselves to the six neutral 28-water clusters. This is to avoid any possible amplification of errors if ionic residues and *a fortiori* metal cations are included, due to the nonpolarizable nature of the force-field. The results of the calculations done with the help of the Chimera software[49] are reported in Figure 8, in which the evolutions of the B97-D, SIBFA, and AMBER interaction energies are compared. The values of ΔE(AMBER) are overestimated by app. 10%. Nevertheless, a satisfactory parallelism with ΔE(B97-D) can be seen. ΔE(AMBER) has also a good r^2 correlation of 0.94 as compared to 0.98 with SIBFA. There are, however, some inversions in the relative stabilities of some complexes, as seen for "*f*", which has the most favorable ΔE(B97-D) and ΔE(SIBFA) values but is second-best with AMBER, next to complex "e" which appears to have an exaggerated stability with respect to the five other ones. We wish to underline that the present kind of comparisons should preferably be considered in the prospect of MD QM/MM simulations, in which the bimetallic Cu/Zn binding site encompassing the metal-binding residues would be treated quantum-mechanically. This results indicate that even in the context of QM/MM approaches there could be a risk with classical force-fields of some bias occurring during MD in which some water networks or arrangements would be incorrectly privileged over the correct ones and possibly predominate during the simulation. This might in turn impact the modes of ligand steering and binding. This would occur despite the fact that, owing to averaging effects, classical MD could in several instances satisfactorily reproduce free energies rather than simple potential energies.

Resorting to *ab initio*-distributed multipoles is an essential asset for accurate reproduction of electrostatics in diverse applications, and in particular for intermolecular interactions. For earlier and recent examples, see, for example, and Refs. Therein [50]. To what an extent could distributed multipoles impact the representation of the molecular electrostatic potentials and fields on accessible surfaces, as compared to the sole monopoles? To address this point, we have determined a distribution of dots around the accessible surface of complex "c" with the 28 waters. The dot distribution was derived with the "discrete" algorithm[25] in which the positions of fictitious waters with effective radii of 0.87 Å instead of 1.87 were optimized around the accessible positions of this complex, then retaining the coordinates of the O atoms. The compression of effective radii was done to increase the density of dots around the surface. This resulted into 700 dots. The electrostatic potential and the square-root of the field were computed with the complete multipole expansion or with the sole monopoles. They were represented on the surface with the help of the VMD software.[51] The electrostatic potential surface has little difference whether computed with multipoles or monopole. It is represented with multipoles as Supporting Information 3 with the same orientation as in Figure 2a. There are some differences in the electrostatic fields, which are represented in Supporting Information 4a–b. While all values are now positive, the distribution of the fields appears more uniform as calculated with the multipoles than with the monopoles. At this stage, it is not possible to draw inferences about the possible implications of this finding.

Conclusions and Perspectives

Cu/Zn-SOD is critical for the protection of cells against free radicals. This renders essential an understanding of its structural and dynamical properties. Cancer cells are even more critically dependent on SOD than healthy cells, thus SOD is an emerging target for the design of antitumor and photosensitizing agents. Highly structured waters in the vicinity of the bimetallic site are an integral part of the protein. It is necessary to ensure that their binding energies to such a region are reliably computed to lend credence to any prediction concerning their organization into networks and the possible lifetimes and interconversion rates of such networks. The QM/MM approach could be considered. However, the large size of the complex to be included in the QM core, and the extension of the water networks at large distances from this core would require a persistent evaluation of the polarization and charge-transfer contributions in the MM region as well. As shown in this study, such contributions should also be demonstrated capable to match their QM counterparts. Until this is demonstrated, and owing to the four-five order of magnitude gains in the QM core, APMM/APMD approaches could be considered as an appealing alternative to QM/MM, particularly in the prospect of MD over very large simulation times. Thus, we have in this study validated the SIBFA procedure against QM computations. We considered first the bimetallic Cu(I)/Zn(II) site, and then networks of structured water molecules in six candidate poses extracted from MD simulations subsequently relaxed by energy-minimization. In the bimetallic site, ΔE(SIBFA) had very close agreement with ΔE(HF), with relative errors $< 3\%$ on considering six possible complexes with net charges varying between 0 and 3. The energy differences increased, however, on passing to the correlated level, that is, comparing ΔE_{tot}(SIBFA) and ΔE(B97-D). Nevertheless, such increases could be partly due to some inherent tendency of B97-D to overestimate the interaction energies with transition metal cations, in as much as MP2, known to overestimate such energies, gave rise to similar ΔE values as ΔE(B97-D).

At the outcome of the MD/EM procedure, six distinct arrays of waters were characterized. The lowest-energy one was the one for which eight waters had the closest overlap with the structural waters identified by X-ray crystallography. It had a dense array of eight waters interposed between Glu131 and Arg141, organized into four networks of two to four H-bonded

waters, some of these being involved in two networks at a time. Some of these waters have very large dipole moments in the range 2.7–3.0 Debye, namely equal to, and larger than ice, namely 2.70 Debye in the context of SIBFA. This attests to the onset of very strong polarization/charge-transfer effects, and is fully consistent with previously published results on the binding of FAK kinase with ionic inhibitors.[22] A network of five linearly H-bonded waters was also identified, running along the Gln137-Thr56 direction, and H-bonded to the dense Glu131-Arg141 network by its first, second, and fifth waters. We have monitored the evolutions of the interaction energies, ΔE(SIBFA) and ΔE_{tot}(SIBFA), along the series of the six complexes a–f, and compared them to the corresponding QM values. In spite of the large size of the complexes used for the validation (301 atoms), ΔE(SIBFA) matched ΔE(HF) (yet uncorrected for BSSE) with relative errors $<3\%$, and its evolution paralleled that of ΔE(HF). With such complexes, a single-point computation with SIBFA is 50,000–100,000 times faster than an HF one. The relative error increased to 4% on comparing ΔE_{tot}(SIBFA) to ΔE(B97-D), owing to some preexisting error within the bimetallic binding, and notwithstanding some possible uncertainties concerning the B97-D procedure applied to transition metal cations. Nevertheless, the corresponding two curves displayed a parallelism equally good to that of ΔE(SIBFA) compared to ΔE(HF). The stabilization energies brought about by the waters (a total of 28 in the model binding site) were also computed. For each complex, this was done by subtracting the total interaction energy in their absence from the one in their presence. The resulting SIBFA and QM energies were in very close agreement, both regarding their numerical values and their evolutions. $E2$, the summed second-order terms, E_{pol} and E_{ct}, contributed about 40% of ΔE(SIBFA). The evolutions of $E1$ and $E2$ reinforced one another to confer to the ΔE(SIBFA) curve a shape matching that of ΔE(HF). Even better agreements obtained, for such stabilizations, on comparing ΔE_{tot} to ΔE(B97-D), the relative error dropping to 2%, as the offset stemming from the bimetallic biding site was removed.

One limitation of this study, common to all MM approaches, whether with rigid or relaxed water geometries, is the fact that proton transfer between water molecules could not be modeled. Such transfers which involve bond breaking and reformation, could only be considered by QM approaches. Because of the intermeshed networks of waters as in complex c, proton transfer could be channeled following different competing pathways. To identify possible privileged proton transfer pathways, it would be appealing for future studies to consider *ab initio* MD studies on moderate-sized complexes, such as c, extracted from prior APMM/APMD simulations on the whole protein.

These results are extremely encouraging in the perspective of very long-time simulations of SOD, which should be enabled by ongoing advances in the integration of the SIBFA potential in a highly efficient and scalable code for MD simulations [Piquemal et al., in preparation]. We, thus, plan to monitor the lifetimes of the polarized structural waters, and whether mutual interconversions of networks could take place. It should also become possible to monitor the diffusion toward the bimetallic binding site of small charged solutes, and these could be channeled preferentially by some of the identified water networks. Thus, would some privileged pathways for approach exist, that would be triggered by the electrostatic potential and field exerted by the bimetallic binding site and residues in its vicinity? Along with standard MD, emerging approaches, such as nonequilibrium MD or Monte-Carlo (MC) [52, and Refs. therein] could be used for that purpose. Such an investigation could similarly be extended to photosensitizing agents and recently discovered antitumor compounds. That is, to what an extent could such compounds mold themselves in the water network and which waters could be replaced and relocated?

We also plan to extend this work to the Cu(II)/Zn(II) site, in which the SIBFA-LF (ligand Field) method[53] will be used to handle the open-shell Cu(II) cation. Finally, this validation results could be used to validate other emerging APMM procedures. For that purpose, the structures of the six model complexes are provided as Supporting Information.

Acknowledgments

The authors sincerely thank the Association Philippe Jabre for funding the PhD research of Krystel El Hage. We wish to thank the Grand Equipement National de Calcul Intensif (GENCI): Institut du Developpement et des Ressources en Informatique Scientifique (IDRIS), Centre Informatique de l'Enseignement Supérieur (CINES), France, project No. x2009-075009), and the Centre de Ressources Informatiques de Haute Normandie (CRIHAN, Rouen, France), project 1998053.

Keywords: superoxide dismutase · structured waters · polarizable molecular mechanics · quantum chemistry

How to cite this article: N. Gresh, K. El Hage, D. Perahia, J.-P. Piquemal, C. Berthomieu, D. Berthomieu *J. Comput. Chem.* **2014**, *35*, 2096–2106. DOI: 10.1002/jcc.23724

Additional Supporting Information may be found in the online version of this article.

[1] J. M. McCord, I. J. Fridovich, *Biol. Chem.* **1969**, *244*, 6049.
[2] L. Raj, T. Ide, A. U. Gurkar, M. Foley, M. Schenone, X. Li, N. J. Tolliday, T. R. Golub, S. A. Carr, A. F. Shamji, A. M. Stern, A. Mandinova, S. L.Schreiber, S. W. Lee, *Nature* **2011**, *475*, 231.
[3] R. Somwar, H. Erdjumen-Bromage, E. Larsson, D. Shum, W. W. Lockwood, G. Yang, C. Sander, O. Ouerfelli, P. J. Tempst, H. Djaballah, H. E. Varmus, *Proc. Natl. Acad. Sci. USA* **2011**, *108*, 16375.
[4] A. Glasauer, L. A. Sena, L. P. Diebold, A. P. Mazar, N. S. Chandell, *J. Clin. Invest.* **2014**, *124*, 117.
[5] M. A. Hough, S. S. Hasnain, *Structure* **2003**, *11*, 937.
[6] J. A. Tainer, E. D. Getzoff, J. S. Richardson, D. C. Richardson, *Nature* **1983**, *306*, 284.
[7] J. A. Tainer, E. D. Getzoff, K. M. Beem, J. S. Richardson, D. C. Richardson, *J. Mol. Biol.* **1982**, *160*, 181.
[8] M. A. Hough, R. W. Strange, S. S. Hasnain, *J. Mol. Biol.* **2000**, *304*, 231.
[9] D. Klug-Roth, I. Fridovich, J. Rabani, *J. Am. Chem. Soc.* **1973**, *95*, 2786.
[10] E. M. Fielden, P. B. Robets, R. C. Bray, D. J. Lowe, G. N. Mautner, G. Rotilio, L. Calabrese, *Biochem. J.* **1974**, *139*, 49.
[11] D. Klug, J. Rabani, I. Fridovich, *J. Biol. Chem.* **1972**, *247*, 4839.

[12] I. Bertini, S. Mangani, M. S. Viezzoli, *Adv. Inorg. Chem.* **1997**, *45*, 127.
[13] M. A. Hough, S. S. Hasnain, *J. Mol. Biol.* **1999**, *287*, 579.
[14] E. Argese, P. Viglino, G. Rotilio, M. Scarpa, A. Rigo, *Biochemistry* **1987**, *26*, 3224.
[15] L. Banci, I. Bertini, C. Luchinat, R. A. Hallewell, *J. Am. Chem. Soc.* **1988**, *110*, 3629.
[16] E. D. Getzoff, D. E. Cabelli, C. L. Fisher, H. E. Parge, M. S. Viezzoli, L. Banci, R. A. Hallewell, *Nature* **1992**, *358*, 347.
[17] M. Falconi, M. Brunelli, A. Pesce, M. Ferrario, M. Bolognesi, A. Desideri, *Proteins* **2003**, *51*, 607.
[18] R. J. F. Branco, P. A. Fernandes, M. J. Ramos, *J. Phys. Chem. B* **2006**, *110*, 1675.
[19] (a) K. Djinovic-Carugo, A. Battistoni, M. T. Carri, F. Polticelli, A. Desideri, G. Rotilio, A. Coda, M. Bolognesi, *FEBS Lett.* **1994**, *349*, 93; (b) K. Djinović-Carugo, F. Polticelli, A. Desideri, G. Rotilio, K. S. Wilson, M. Bolognesi, *J. Mol. Biol*. **1994**, *240*, 179.
[20] P. J. Hart, M. M. Balbimie, N. L. Ogihara, A. Nersissian, M. S. Weiss, J. S. Valentine, D. Eisenberg, *Biochemistry* **1999**, *38*, 2167.
[21] L. Bijeire, B. Elias, J.-P. Souchard, E. Gicquel, C. Moucheon, A. Kirsch-de Mesmaeker, P. Vicendo, *Biochemistry* **2006**, *45*, 6160.
[22] B. de Courcy, J.-P. Piquemal, C. Garbay, N. Gresh, *J. Am. Chem. Soc.* **2010**, *132*, 3312.
[23] N. Gresh, B. de Courcy, J. P. Piquemal, J. Foret, S. Courtiol-Legourd, L. Salmon, *J. Phys. Chem. B* **2011**, *115*, 8304.
[24] Accelrys software, San Diego, California. http://accelrys.com.
[25] P. Claverie, J.-P. Daudey, J. Langlet, B. Pullman, D. Piazzola, M.-J. Huron, *J. Phys. Chem.* **1978**, *82*, 405.
[26] W. C. Swope, H. C. Andersen, P. H. Berens, K. R. Wilson, *J. Chem. Phys.* **1982**, *76*, 637.
[27] F. Liparini, L. Lagardere, B. Stamm, E. Cances, M. Schnieders, P. Ren, Y. Maday, J.-P. Piquemal, *J. Chem. Theory Comput.* **2014**, *10*, 1638.
[28] J.-P. Ryckaert, G. Ciccoti, H. J. C. Berendsen, *J. Comput. Phys.* **1977**, *23*, 327.
[29] H. J. C. Berendsen, J. P. M. Postma, W. F. van Gusnteren, A. DiNola, J. R. Haak, *J. Chem. Phys.* **1984**, *81*, 3684.
[30] G. A. Evangelakis, J. P. Rizos, I. E. Lagaris, I. N. Demetropoulos, *Comput. Phys. Commun.* **1987**, *46*, 401.
[31] F. Vigné-Maeder, P. Claverie, *J. Chem. Phys.* **1988**, *88*, 4934.
[32] D. R. Garmer, W. J. Stevens, *J. Phys. Chem.* **1989**, *93*, 8263.
[33] (a) W. J. Stevens, H. Basch, M. Krauss, *J. Chem. Phys.* **1984**, *81*, 6026; (b) W. J. Stevens, M. Krauss, H. Basch, P. G. Jasien, *Can. J. Chem*. **1992**, *70*, 612.
[34] W. J. Stevens, W. Fink, *Chem. Phys. Letts.* **1987**, *139*, 15.
[35] M. W. Schmidt, K. K. Baldridge, J. A. Boatz, S. T. Elbert, M. S. Gordon, J. H. Jensen, S. Koseki, N. Matsunaga, K. A. Nguyen, S. Su, T. L. Windus, M. Dupuis, J. A. Montgomery, *J. Comput. Chem.* **1993**, *14*, 1347.
[36] S. Grimme, *J. Comput. Chem.* **2006**, *27*, 1787.
[37] S. Grimme, J. Antony, S. Ehrlich, H. Krieg, *J. Chem. Phys.* **2010**, *132*, 154104.
[38] M. J. Frisch, G. W. Trucks, H. B. Schlegel, G. E. Scuseria, M. A. Robb, J. R. Cheeseman, G. Scalmani, V. Barone, B. Mennucci, G. A. Petersson, H. Nakatsuji, M. Caricato, X. Li, H. P. Hratchian, A. F. Izmaylov, J. Bloino, G. Zheng, J. L. Sonnenberg, M. Hada, M. Ehara, K. Toyota, R. Fukuda, J. Hasegawa, M. Ishida, T. Nakajima, Y. Honda, O. Kitao, H. Nakai, T. Vreven, J. A. Montgomery, Jr., J. E. Peralta, F. Ogliaro, M. Bearpark, J. J. Heyd, E. Brothers, K. N. Kudin, V. N. Staroverov, R. Kobayashi, J. Normand, K. Raghavachari, A. Rendell, J. C. Burant, S. S. Iyengar, J. Tomasi, M. Cossi, N. Rega, N. J. Millam, M. Klene, J. E. Knox, J. B. Cross, V. Bakken, C. Adamo, J. Jaramillo, R. Gomperts, R. E. Stratmann, O. Yazyev, A. J. Austin, R. Cammi, C. Pomelli, J. W. Ochterski, R. L. Martin, K. Morokuma, V. G. Zakrzewski, G. A. Voth, P. Salvador, J. J. Dannenberg, S. Dapprich, A. D. Daniels, Ö. Farkas, J. B. Foresman, J. V. Ortiz, J. Cioslowski, D. J. Fox, Gaussian 09, Revision D.01; Gaussian, Inc.: Wallingford, CT, **2009**.
[39] S. F. Boys, F. Bernardi, *Mol. Phys.* **1970**, *19*, 553.
[40] (a) E. R. Johnson, S. Keinan, P. Mori-Sanchez, J. Contreras-Garcia, A. J. Cohen, W. T. Yang, *J. Am. Chem. Soc.* **2010**, *132*, 6498; (b) J. Contreras-Garcia, E. R. Johnson, S. Keinan, R. Chaudret, J.-P. Piquemal, D. Beratan, W. Yang, *J. Chem. Theory Comput*. **2011**, *7*, 625.
[41] (a) N. Gresh, J.-P. Piquemal, M. Krauss, *J. Comput. Chem.* **2005**, *26*, 1113; (b) J. Antony, J.-P. Piquemal, N. Gresh, *J. Comput. Chem*. **2005**, *26*, 1131.
[42] N. Gresh, N. Audiffren, J.-P. Piquemal, J. de Ruyck, M. Ledecq, J. Wouters, *J. Phys. Chem. B* **2010**, *114*, 4884.
[43] D. R. Garmer, N. Gresh, B.-P. Roques, *Proteins: Struct. Funct. Genet.* **1998**, *31*, 42.
[44] G. Tiraboschi, N. Gresh, C. Giessner-Prettre, L. G. Pedersen, D. W. Deerfield, *J. Comput. Chem.* **2000**, *21*, 1011.
[45] N. Gresh, C. Policar, C. Giessner-Prettre, *J. Phys. Chem. A* **2002**, *106*, 5660.
[46] P. Hobza, J. Sponer, *Chem. Rev.* **1999**, *99*, 3247.
[47] J.-P. Piquemal, R. Chelli, P. Procacci, N. Gresh, *J. Phys. Chem. A* **2007**, *111*, 8170.
[48] W. D. Cornell, P. Cieplak, C. I. Bayly, I. R. Gould, K. M. Merz, Jr., D. M. Ferguson, D. C. Spellmeyer, T. Fox, J. W. Caldwell, P. A. Kollman, *J. Am. Chem. Soc.* **1995**, *117*, 5179.
[49] E. F. Pettersen, T. D. Goddard, C. C. Huang, G. S. Couch, D. M. Greenblatt, E. C. Meng, *T. E. Ferrin. J. Comput. Chem.* **2004**, *25*,1605.
[50] (a) N. Gresh, P. Claverie, A. Pullman, *Int. J. Quantum Chem. Symp.* **1979**, *13*, 243; (b) A. J. Stone, S. L. Price, *J. Phys. Chem*. **1988**, *92*, 3325; (c) W. A. Sokalski, M. Shibata, R. Rein, R. L. Ornstein, *J. Comput. Chem*. **1992**, *13*, 883; (d) N. Gresh, H. Guo, D. R. Salahub, B. P. Roques, S. A. Kafafi, *J. Am. Chem. Soc*. **1999**, *121*, 7885; (e) P. Soederhjelm, J. W. Krog, G. Karlstrom, U. Ryde, R. Lindh, *J. Comput. Chem*. **2007**, *28*, 1083; (f) M. Devereux, N. Plattner, M. Meuwly, *J. Phys. Chem*. **2009**, *113*, 13199; (g) P. Ren, C. Wu, J. W. Ponder, *J. Chem Theory Comput*. **2011**, *7*, 3143; (h) C. Cramer, T. Bereau, A. Spinn, K. R. Liedl, P. Gedeck, M. Meuwly, *J. Chem. Inf. Model*. **2013**, *53*, 3410; (i) M. S. Gordon, Q. A. Smith, P. Xu, L. V. Slipchenko, *Ann. Rev. Phys. Chem*. **2013**, *64*, 553.
[51] W. Humphrey, A. Dalke, K. Schulten, *J. Mol. Graph. Model.* **1996**, *14*, 33.
[52] P. Nicolini, D. Frezzato, C. Gellini, M. Bizzarri, R. Chelli, *J. Comput. Chem.* **2013**, *18*, 1561.
[53] J.-P. Piquemal, B. W. Hubbard, N. Fey, R. Deeth, N. Gresh, C. Giessner-Prettre, *J. Comput. Chem.* **2003**, *24*, 1963.

Received: 19 June 2014
Revised: 9 August 2014
Accepted: 12 August 2014
Published online on 11 September 2014